

Article

Dual Cross-Linked Carboxymethyl Sago Pulp-Gelatine Complex Coacervates for Sustained Drug Delivery

Saravanan Muniyandy ^{1,*}, Thenapakiam Sathasivam ^{1,†}, Anand Kumar Veeramachineni ^{2,†} and Pushpamalar Janarthanan ^{2,†}

¹ School of Pharmacy, Monash University Malaysia, Jalan Lagoon Selatan, Bandar Sunway 47500, Selangor Darul Ehsan, Malaysia; E-Mail: thena5920@gmail.com

² School of Science, Monash University Malaysia, Jalan Lagoon Selatan, Bandar Sunway 47500, Selangor Darul Ehsan, Malaysia; E-Mails: akvee1@student.monash.edu (A.K.V.); pushpa.janarthanan@monash.edu (P.J.)

† These authors contributed equally to this work.

* Author to whom correspondence should be addressed; E-Mail: Saravanan.muniyandy@monash.edu; Tel.: +603-5514-4926; Fax: +603-5514-6323.

Academic Editor: João F. Mano

Received: 23 April 2015 / Accepted: 29 May 2015 / Published: 15 June 2015

Abstract: In the present work, we report for the first time the complex coacervation of carboxymethyl sago pulp (CMSP) with gelatine for sustained drug delivery. Toluene saturated with glutaraldehyde and aqueous aluminum chloride was employed as cross-linkers. Measurements of zeta potential confirm neutralization of two oppositely charged colloids due to complexation, which was further supported by infrared spectroscopy. The coacervates encapsulated a model drug ibuprofen and formed microcapsules with a loading of 29%–56% w/w and an entrapment efficiency of 85%–93% w/w. Fresh coacervates loaded with drug had an average diameter of $10.8 \pm 1.93 \mu\text{m}$ ($n = 3 \pm \text{s.d.}$). The coacervates could encapsulate only the micronized form of ibuprofen in the absence of surfactant. Analysis through an optical microscope evidenced the encapsulation of the drug in wet spherical coacervates. Scanning electron microscopy revealed the non-spherical geometry and surface roughness of dried drug-loaded microcapsules. X-ray diffraction, differential scanning calorimetry and thermal analysis confirmed intact and crystalline ibuprofen in the coacervates. Gas chromatography indicated the absence of residual glutaraldehyde in the microcapsules. Dual cross-linked

microcapsules exhibited a slower release than mono-cross-linked microcapsules and could sustain the drug release over the period of 6 h following Fickian diffusion.

Keywords: complex coacervation; ibuprofen; gelatine; carboxymethyl sago pulp; sustained release; microencapsulation

1. Introduction

One of the most crucial innovations in recent years is the conversion of plant waste into useful products. Sago palm (*Metroxylon sagu*) is found abundantly in Malaysia (particularly in Johor Bharu and Sarawak) and has a rich source of starch that serves as one of the most important food sources for communities across the globe. Carboxymethyl sago pulp (CMSP), a semisynthetic polymer, was synthesized from Malaysian sago biomass and characterized by Pushpamalar *et al.*, 2006 [1,2]. CMSP typically contains [3] sodium carboxymethyl hemicellulose (38%–40%) and sodium carboxymethyl alpha cellulose (23%–25%), along with lignin (28%–30%) and non-starch polysaccharides (3%–5%). Recently, CMSP bead was exploited for colon targeted drug delivery of 5-aminosalicylic acid [4]. These CMSP beads were prepared by ionotropic gelation followed by radiation cross-linking. This method yields larger particles and also need radiation facilities. In addition radiation cross-linking might not suit radiation sensitive materials. In contrast, complex coacervation does not require sophisticated equipment and can produce smaller particles. Hence, in the present work, complex coacervation of CMSP with gelatin is attempted for microencapsulation and sustained drug delivery.

Complex coacervation is one of the oldest and simplest methods [5] of encapsulating drugs for sustained drug delivery. The process is simple and does not require high temperatures or toxic solvents. Hence, it is also employed in the encapsulation of delicate materials such as protein [6] and human cells [7]. Coacervation refers to a phase separation process, and complex coacervation involves the complexation between two oppositely charged colloids to yield a colloid-rich region that is used to coat the core (drug) particles. Anionic polysaccharides [8], such as acacia, pectin, alginate and carboxymethyl cellulose, were used with cationic protein molecules, such as gelatine, casein, albumin and chitosan, to produce a complex coacervation. The concentration of colloids, physicochemical properties of the drug being encapsulated, cross-linking agents and pH at which coacervation takes places are the most important parameters to obtain the final product [9]. Complex Coacervation also established using oppositely charged polyelectrolytes [10,11] as well as polypeptides [12]. Parameters such as salt concentration, chirality/hydrogen bonding and molecular weight also have a significant effect on complex coacervation [13,14]. Ibuprofen is a non-steroidal anti-inflammatory drug primarily used for relief of symptoms from arthritis, primary dysmenorrhea, fever, and as an analgesic, especially when an inflammatory component is part of the illness [15]. In conventional therapy, frequent administration of ibuprofen is required due to its short biological half-life (1.9 to 2.2 h), which may lead to fluctuation in plasma drug profile. Excessive use of ibuprofen has been related to an increase in hearing loss [16] and an elevated risk of myocardial infarction [17]. The short biological half-life and associated side effects make ibuprofen a suitable candidate for controlled-release formulation.

In the present investigation, ibuprofen is encapsulated in CMSP/gelatine complex coacervates using glutaraldehyde as the cross-linking agent. A few select formulations were also treated with aluminum chloride to sustain the release further. CMSP/gelatine coacervates were characterized by zeta-potential and Fourier-transform infrared spectroscopy (FT-IR) to confirm complex formation. Drug-loaded coacervates were evaluated for loading/entrapment efficiency, particle size/distribution, optical and field emission scanning electron microscopy (FE-SEM), differential scanning calorimetry (DSC), thermogravimetric analysis (TGA), X-ray diffraction (XRD), residual glutaraldehyde and *in vitro* release.

2. Experimental Section

2.1. Materials

Sago biomass was obtained from PPES Sago Industries Sendirian Berhad (Mukah, Dalat, Sarawak, Malaysia). Ibuprofen was purchased from Lianyungang Zhongyi International Trade Co. Ltd. (Lianyungang, China). Gelatine from porcine skin (Type A, 300 bloom strength) was obtained from Sigma-Aldrich (St. Louis, MO, USA). Glutaraldehyde (25% aqueous solution), aluminum chloride, sodium lauryl sulfate (SLS) and other chemicals used in this study were of analytical grade, obtained from HmbG chemicals and Bumi-Pharma Sdn. Bhd. (Balakong, Malaysia).

2.2. Preparation of Carboxymethyl Sago Pulp

Carboxymethyl sago pulp (CMSP) with a degree of substitution of 0.4, an intrinsic viscosity of 184 dL/g and a molecular weight of 76,000 g/mol was synthesized from sago biomass using the Williamson ether synthesis, as described in previous publications [1–3]. Briefly, 20 g of the sago waste was transferred into a 1000-mL Erlenmeyer flask and suspended in 640 mL of hot distilled water. Four milliliters of glacial acetic acid and 6 g of sodium chlorite were subsequently added. The mixture was later heated at 70 °C for 3 h and then filtered and washed with cold distilled water. The resulted white residue (sago pulp) was dried in the oven to its constant weight.

Five grams of the sago pulp was added into 100 mL of isopropanol and 10 mL of 30% sodium hydroxide. The mixture was stirred for an hour at 160 rpm in a thermo stated water bath with a horizontal shaker (Model SW22, Julabo, Germany). The carboxymethylation reaction was started by adding 3 g of sodium monochloroacetate to the reaction mixture. Then, the stirring (160 rpm) was continued at 45 °C for 3 h. The mixture was filtered and suspended in 300 mL of methanol overnight and neutralized with glacial acetic acid. The mixture was filtered again and washed thoroughly with 150 mL of ethanol to remove undesirables and was dried in an oven at 60 °C.

2.3. Preparation of Micronized Ibuprofen

Micronization of ibuprofen native particles was performed using a modified version of the solvent/anti-solvent precipitation method reported previously [18]. Native ibuprofen was dissolved in isopropanol until saturation. The alcohol solution was added dropwise into 0.5% w/v sodium lauryl sulfate (SLS) and was homogenized using an IKA T25 Digital Ultra-Turrax (IKA, Wilmington, DE, USA) at 12,000 rpm for 3 min. Then, the resulting micronized ibuprofen (m-INN) suspension was collected by centrifugation at 15,300 rpm for 20 min and washed several times with distilled water to

remove SLS. Finally, m-INN was oven-dried at 35 °C for 24 h and sieved through a 500- μ m sieve. Dried m-INN particles were transferred to a glass vial and closed using a rubber cap before being stored in a desiccator.

2.4. Encapsulation of m-INN Using CMSP/Gelatine Complex Coacervation

As shown in Table 1, different batches of m-INN-loaded CMSP-gelatine microcapsules were formulated as follows. Aqueous solutions of 2% w/v CMSP and gelatine solutions were prepared separately by stirring at 300 rpm using a magnetic stirrer at 45 °C. The pH of the individual solution was adjusted to 5 using 10% v/v acetic acid. The required quantity of the m-INN was dispersed throughout the CMSP solution using ultrasonication (Hielscher UIP500hd, Teltow, Germany, 60% amplitude for 4 min). Then, an equal volume of gelatine solution was added and stirred at 300 rpm for 15 min. The pH was adjusted to 3.8 using 1% v/v acetic acid to induce complex coacervation. The coacervate was allowed to equilibrate by continuous stirring at 160 rpm, and the mixture was slowly cooled to reach room temperature. Microcapsules were cross-linked by slow addition of toluene saturated with glutaraldehyde (GST) and stirred for 3 h at 5 °C to harden the walls. Then, the cross-linking was quenched by adding 20 mL of 10% w/v sodium metabisulfite. The microcapsules were allowed to sediment, and the supernatant was discarded. The sediments were washed with 50 mL of 50%, 75%, and 99% v/v isopropyl alcohol and dried at room temperature for 24 h. To further cross-link with aluminum chloride (AlCl₃), new batches of A, D and, E were stirred with 200 mL of 5% w/v of AlCl₃ at 300 rpm for 15 min before washing with isopropanol. Similarly, unloaded coacervates were also prepared without the addition of the m-INN.

Table 1. Physicochemical parameters of m-INN loaded CMSP-gelatine microcapsules prepared by complex coacervation.

Formulation Code	CMSP (g)	Gelatine (g)	m-INN (g)	GST (mL)	Drug Loading (%) (n = 3 \pm s.d.)		Entrapment Efficiency (%) (n = 3 \pm s.d.)
					Theoretical	Experimental	
A	2	2	2	10	33.33	29.54 \pm 0.71	88.62 \pm 2.15
B	2	2	4	10	50	44.72 \pm 4.03	89.44 \pm 8.06
C	2	2	6	10	60	56.09 \pm 2.31	93.48 \pm 3.85
D	2	2	2	20	33.3	28.22 \pm 0.84	84.66 \pm 2.53
E	2	2	2	30	33.3	30.07 \pm 0.55	90.21 \pm 1.66

2.5. Drug Loading and Entrapment Efficiency

Approximately 100 mg of samples were placed in 100 mL of 2 N NaOH and stirred for 24 h at room temperature. Then, the samples were filtered using Whatman filter paper, and the amount of ibuprofen was estimated at 264 nm [19] using a Shimadzu UV-visible spectrophotometer (UVmini-1240, Shimadzu, Kyoto, Japan). A known concentration of ibuprofen solution (2 N NaOH) premixed with unloaded coacervates was used as a reference standard. The theoretical percentage of drug loading (TDL) was calculated using the following equation.

$$TDL = (\text{Weight of drug added} / \text{Weight of polymers and drug added}) \times 100 \quad (1)$$

The percentage of drug entrapment efficiency (*DEE*) was calculated according to the following equation [20].

$$DEE = (\text{Experimental drug loading} / \text{Theoretical drug loading (TDL)}) \times 100 \quad (2)$$

2.6. Particle Size Analysis and Zeta Potential Measurement

Particle size analysis (Mastersizer 3000, Malvern, UK) was performed on fresh samples, and size distributions were plotted using the Mastersizer 3000 software. Size distribution of native ibuprofen, m-INN and CMSP/gelatine complex coacervates with and without m-INN were measured after 30 s of sonication. An average of three scans was used for size determination. The surface charges of 2% w/v CMSP and gelatine at pH 3.8, 5 and 7, along with complex coacervates at pH 3.8, were measured by a Zetasizer (Nano ZS90, Malvern, Worcestershire, UK) using a fold capillary cuvette (Folded Capillary Cell-DTS 1060, Malvern, Worcestershire, UK).

2.7. Fourier Transform Infrared Spectroscopy

The infrared spectrums of the samples were measured between 600 and 3800 cm^{-1} in a Varian 640-IR FTIR spectrophotometer (Agilent Technologies, Santa Clara, CA, US) using an attenuated total reflection accessory.

2.8. Optical and Field Emission Scanning Electron Microscopy

An optical microscope (Olympus BX50, Tokyo, Japan) was used to obtain images of fresh coacervate and dried samples. A field emission scanning electron microscope (SU8010, Hitachi, Krefeld, Germany) was used to observe surface morphology and the shape of the dried microcapsules. The samples were fixed in stubs using double-faced copper adhesive tape and were coated with a thin layer of platinum using a Q150R S rotary-pumped sputter coating system (Quorum Technologies, East Sussex, UK) before being observed.

2.9. X-Ray Diffractometry

An X-ray diffraction apparatus (InXitu BTXII, Olympus, Waltham, MA, USA) was used to obtain the X-ray diffraction patterns of the samples. Each sample was ground to produce particles less than 75 μm in size and homogeneously mixed. Approximately 15 mg of each sample was loaded into the apparatus via the sample spinner assembly, and a 90-min acquisition produced the diffractograms over a 2θ range. The analysis was performed with a cobalt target X-ray tube operating at 30 kV and 330 μA .

2.10. Differential Scanning Calorimetry

Differential scanning calorimetry (DSC) analyses were performed in a temperature range from 25 to 120 $^{\circ}\text{C}$ on a DSC 4000 (Perkin Elmer, Waltham, MA, USA). Approximately 5 mg of each respective sample was weighed and sealed into the aluminum pans. The heating rate was 5 $^{\circ}\text{C}/\text{min}$, and the nitrogen flow rate was 20 mL/min.

2.11. Thermogravimetric Analysis

The thermal properties of samples were analyzed on a thermogravimetric analyzer (TGA Q50, TA Instruments, New Castle, DE, USA). Three milligrams of sample was heated at the rate of 25 °C/min up from 20–600 °C under constant nitrogen flow.

2.12. In Vitro Release

The *in vitro* release study was performed using 200 mL of phosphate buffer (pH 7.4), as the dissolution medium in a 250-mL flask [19]. The flasks were kept in a water bath shaker (100 rpm and 37.0 ± 0.5 °C) and microcapsules containing the equivalent of 100 mg of ibuprofen were added to the buffer. Five-milliliter aliquots were withdrawn from the flask at different intervals, and the same volume of the fresh phosphate buffer media was replaced. The amount of ibuprofen in the samples was measured at 264 nm using a spectrophotometer (UVmini-1240, Shimadzu, Kyoto, Japan).

2.13. Test for Residual Glutaraldehyde

Approximately 0.5 g of each sample was extracted with 10 mL of isopropyl alcohol by vigorous shaking for 24 h. The extract was filtered, and 0.5 μ L of filtrate was injected into the chromatographic system column for glutaraldehyde determination [21]. The Clarus 580 GC gas chromatograph model (Perkin Elmer, Waltham, Massachusetts, USA) was equipped with a flame ionization detector and a carbowax column (Carbowax-20M, 10%, 3 m, 1/800, 80/100 meshes). Hydrogen at a flow-rate of 4 mL/min was employed as a carrier gas. The operating temperatures were as follows: detector, 200 °C; and oven, initial 50 °C with 2 min hold time and a ramp of 15 °C/min up to 200 °C.

3. Results and Discussion

3.1. Complex Coacervation and m-INN Encapsulation

The pH at which coacervation occurs is a critical point in the encapsulation process by complex coacervation. The coacervates were produced when the pH was adjusted to 3.8 in the CMSP/gelatine mixture. At that point, gelatine has a maximum positive charge, and CMSP has a maximum negative charge. These charges induce complexation followed by phase separation. The attempt to encapsulate native ibuprofen particles failed because the particles were larger than the coacervates. The inclusion of a non-ionic surfactant (Tween 20) in the system was attempted during the coacervation to obtain spherical and less aggregated microcapsules. The presence of Tween 20 produced spherical and small size coacervates. It also formed a protective barrier between the drug particle and coacervate, thus preventing the coalescence of coacervates around the drug particles. To successfully coalesce the coacervates, the native ibuprofen particle size was reduced to produce m-INN. The CMSP-gelatine coacervates were then able to coalesce around the m-INN to form microcapsules only in the absence of surfactant.

As shown in Table 1, the DEE of the batches of microcapsules was 85%–93% *w/w*, indicating good encapsulation efficiency; however, some of the drug was lost during washing and recovery. At a higher drug to polymer ratio (Formulation B and C), the DEE was slightly high; this increase in DEE could be due to the development of multinucleate microcapsules prepared at higher theoretical loading. Normally,

higher cross-linking would reduce drug loading due to the drug particles being pushed out of the microcapsules by the closer arrangement of the highly cross-linked polymeric network. In contrast, as seen in Table 1, the higher degree of cross-linking did not significantly change the drug loading. This discrepancy could be due to the poor solubility of ibuprofen at coacervation pH along with the formation of multinucleate microcapsules. In addition, a higher amount of cross-linking agent caused inter-particle cross-linking and produced larger aggregated particles. Glutaraldehyde and aluminum chloride were used as cross-linking agents. Glutaraldehyde and aluminum cross-linked the gelatine and carboxyl group of CMSP in the complex coacervates, respectively. Dual cross-linking might be more beneficial than mono to get prolonged release.

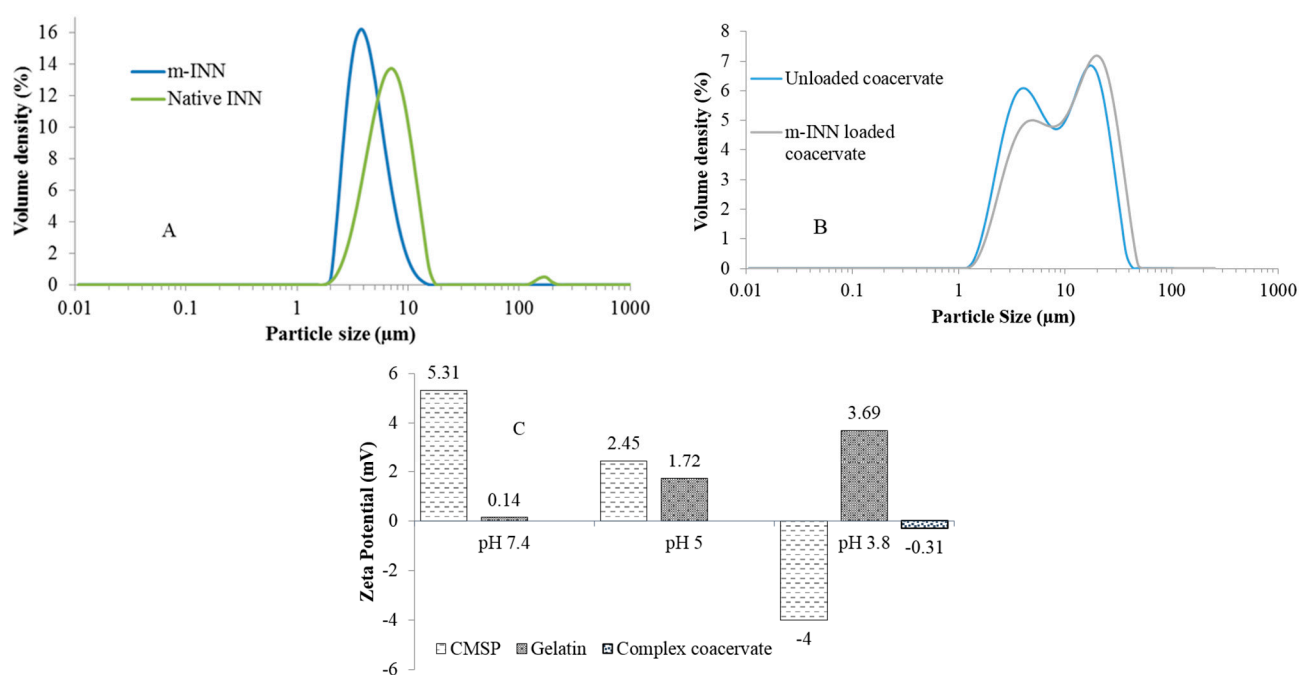


Figure 1. (A) Particle size distribution (log scale) of native and micronized ibuprofen (INN); (B) The size distribution (log scale) of unloaded and drug loaded coacervates; and (C) The zeta potential of CMSP, gelatine and complex coacervates.

3.2. Particle Size and Zeta Potential Analysis

The micronization of native ibuprofen resulted in size reduction as well as narrow size distribution, as indicated in Figure 1A. The size of the micronized particles was within the range of 1 to 20 μm, whereas the native ibuprofen particles were in the range of 1 to 200 μm. The average sizes of native ibuprofen and micronized ibuprofen particles were $8.88 \pm 1.56 \mu\text{m}$ and $6.67 \pm 1.21 \mu\text{m}$, respectively ($n = 3 \pm \text{s.d.}$). As seen in Figure 1B, the size distribution of the freshly prepared unloaded and ibuprofen loaded complex coacervates is approximately the same. The size distribution of unloaded and 30% w/w drug loaded complex coacervate particles were in the range of 1–48 μm and 1–55 μm, respectively, with an average size of $8.25 \pm 1.78 \mu\text{m}$ and $10.8 \pm 1.93 \mu\text{m}$, respectively ($n = 3 \pm \text{s.d.}$). As shown in Figure 1B, the drug loading did not affect the size or size distribution. Microcapsules with higher loading (45% and 56% w/w) have also produced similar size distributions. This result could be due to the narrow size distribution of the m-INN employed in the encapsulation process. The size distribution of dried

microcapsules was discontinued due to particle aggregation, which was difficult to disperse in spite of ultrasonication. To validate the complexation between CMSP and gelatine, the zeta potential of individual colloids at different pH values as well as at the pH of coacervation was recorded and presented in Figure 1C. The zeta potential of CMSP was reduced from 5.31 to -4.00 mV with decreasing pH from 7.4 to 3.8. The initial higher zeta potential is due to the presence of excess sodium counter ions. The zeta potential decreased when pH was adjusted to 3.8 due to neutralization of counter ions and the ionization of carboxylic acid groups (pK_a 3.8–4.2) in CMSP [4]. The zeta potential value of gelatine shifts from 0.14 to 3.69 mV with a decrease in pH. At pH 3.8, the net charges of CMSP and gelatine were -4 and 3.69 mV, respectively. The zeta potential of complex coacervates formed at pH 3.8 was -0.31 mV, indicating the presence of charge neutralization due to complexation. The small negative value indicates the presence of excess negative CMSP ions. The neutralization of the charges confirmed formation of a complex between the two colloids. Moreover, an excess of carboxyl groups allows further cross-linking with aluminum chloride.

3.3. Fourier Transform Infrared Spectroscopy Studies

The IR spectrum of CMSP showed a broad peak at 3326 cm^{-1} due to the stretching vibration of the $-\text{OH}$ group (Figure 2a). The peak at 2897 cm^{-1} is due to $\text{C}-\text{H}$ stretching vibrations. The presence of a strong absorption band at 1596 cm^{-1} confirms the presence of a $-\text{COO}^-$ group and acts as evidence of the carboxylation of sago pulp. The bands at 1417 and 1319 cm^{-1} are for CH_2 scissors and OH bending vibrations, respectively. The broad bands from 1000 to 1200 cm^{-1} were due to sugar ring absorption [2,22–24]. The FT-IR spectrum of gelatine (Figure 2b) shows characteristic peaks at 3297 cm^{-1} due to $\text{O}-\text{H}$ stretching vibrations. Peaks at 3080 , 2963 and 2840 cm^{-1} revealed the amino groups. Other notable peaks in gelatine were at 2963 cm^{-1} ($\text{C}-\text{H}$ stretching of alkenes), 2846 cm^{-1} ($\text{C}-\text{H}$ stretching of alkanes), 1637 cm^{-1} (amide-I CO and CN stretching) and 1545 cm^{-1} (amide-II). The peaks observed in gelatine at 1082 and 1017 cm^{-1} are due to the $\text{C}-\text{O}$ stretching of carboxylic acids and the $\text{C}-\text{N}$ stretching of amines, respectively [25]. The CMSP has a free carboxyl group that imparts a negative charge to these molecules, whereas gelatine has a positive charge at acidic pH due to the presence of amino groups. Most of the peaks of coacervate resemble the gelatine spectrum. The weak peaks of the free amino group at 2840 cm^{-1} in gelatine disappeared (Figure 2c) in the CMSP/gelatine complex coacervate. A characteristic peak for an amide group in the region of $800\text{--}600\text{ cm}^{-1}$ appeared in the complex coacervate (out of the plane, $-\text{N}-\text{H}$ wagging of primary and secondary amide) and confirmed the formation of the complex due to the reaction between the amino groups of gelatine and the carboxylic group of CMSP. The spectrum of complex coacervates resembles the gelatine-pectin coacervate reported by Saravanan and Rao, 2011 [9]. Moreover, a less intensive peak of a sugar ring appeared at 1040 cm^{-1} in the complex coacervate and indicated the association of CMSP with gelatine. These observations along with zeta potential measurements confirm the complexation of CMSP and gelatine.

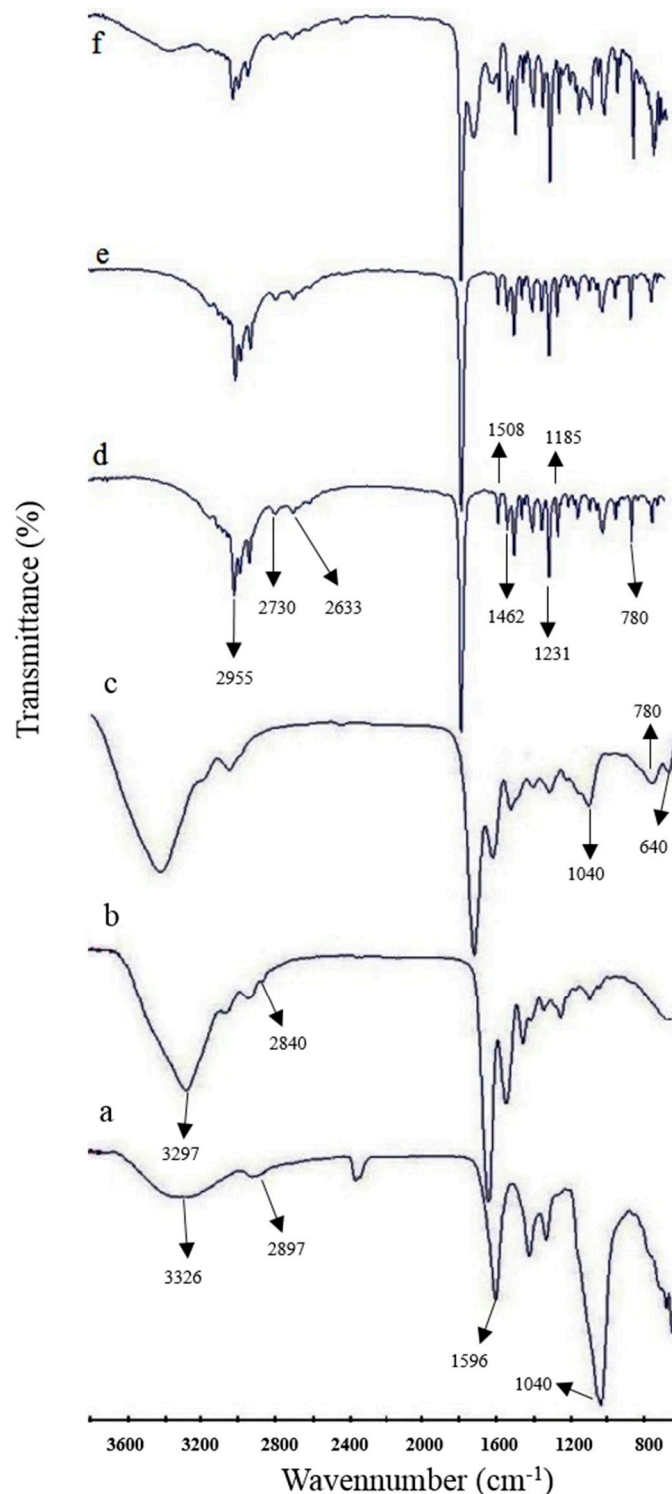


Figure 2. FT-IR spectrum of CMSP (a), gelatine (b), CMSP-gelatine complex coacervate (c), native ibuprofen (d), m-INN (e) and 45% m-INN loaded in CMSP-gelatine microcapsules (f).

The FTIR spectrum of raw ibuprofen (Figure 2d) shows two characteristic bands of medium intensity at 2633 cm^{-1} and 2731 cm^{-1} , corresponding to the stretching vibration of the cyclic dimerized hydroxyl groups. The bending -OH absorption at 1231 cm^{-1} reveals free hydroxyl groups, and a peak at 1185 cm^{-1} indicates C-O stretching vibrations. Characteristic peaks at 1710 and 2955 cm^{-1} were observed for C=O

and –OH stretching, respectively, for the carboxylic acid group [19] in the ibuprofen. The peaks at 1508, 1462 and 780 cm^{-1} are associated with the vibration in the skeleton of benzene. The multiple spectral lines observed around 3100–2900 cm^{-1} are attributed to C–H stretching vibrations [26]. These characteristic peaks of raw ibuprofen presented in the spectrum of the m-INN (Figure 2e), indicating the intact nature of ibuprofen after micronization. The FTIR spectrum of drug-loaded CMSP-gelatine coacervates (Figure 2f) showed the characteristic peaks of ibuprofen and confirmed successful encapsulation of the drug.

3.4. X-Ray Diffractometry

The X-ray diffraction (XRD) patterns of micronized ibuprofen (Figure 3a) showed numerous characteristic sharp and intense peaks at 2° , 16° , 18° , 20° and 22° , revealing a crystalline state of the drug [27]. The XRD of complex coacervates (Figure 3b) did not display any sharp peaks and suggests an amorphous state of the encapsulating material. The peaks of ibuprofen in the XRD of loaded microcapsules (Figure 3c) confirmed the crystalline form of the encapsulated drug. As drug loading increased, the peak intensities also increased (Figure 3c–e) proportionately.

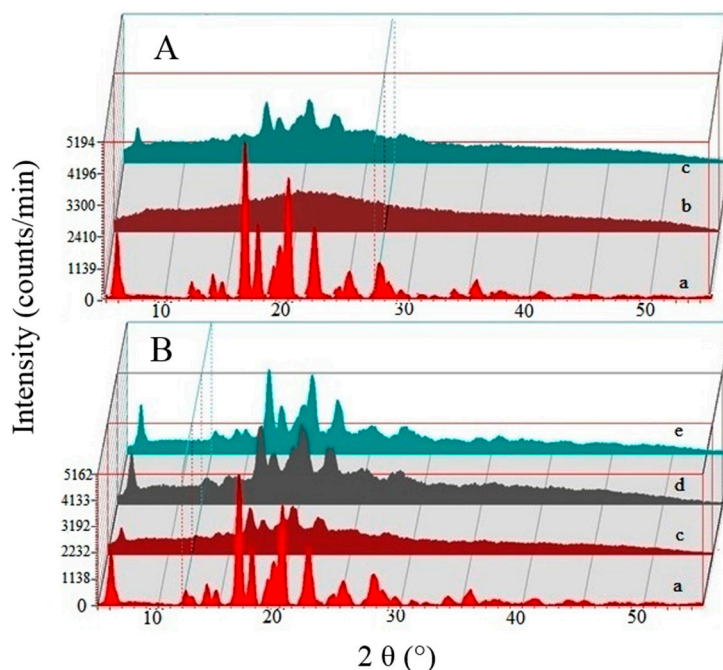


Figure 3. X-ray diffractograms of micronized ibuprofen (a), unloaded (b), 30 (c), 45 (d) and 56% w/w (e) m-INN-loaded complex coacervate. (A) shows crystalline nature of ibuprofen (a) and amorphous nature of unloaded coacervates (b); and (B) shows proportional increase in crystalline peak intensity with increasing ibuprofen content.

3.5. Differential Scanning Calorimetry

The DSC thermogram of CMSP-gelatine coacervates did not show any definite peaks and revealed its amorphous nature (Figure 4A(a)). The m-INN (Figure 4A(b)) and physical mixture (1:1:1 ratio) of m-INN/CMSP-gelatine (Figure 4A(c)) shows an endothermic peak at ibuprofen's melting point (71.8°C), indicating the crystalline nature of the drug and absence of a drug-polymer interaction [19]. The drug-loaded coacervate showed a sharp endothermic peak at 72°C , revealing the crystalline state

of ibuprofen. The intensity of this peak proportionally increased (Figure 4B(d–f)) with drug loading. Along with XRD, DSC results confirm the crystalline nature of the intact ibuprofen within the microcapsules.

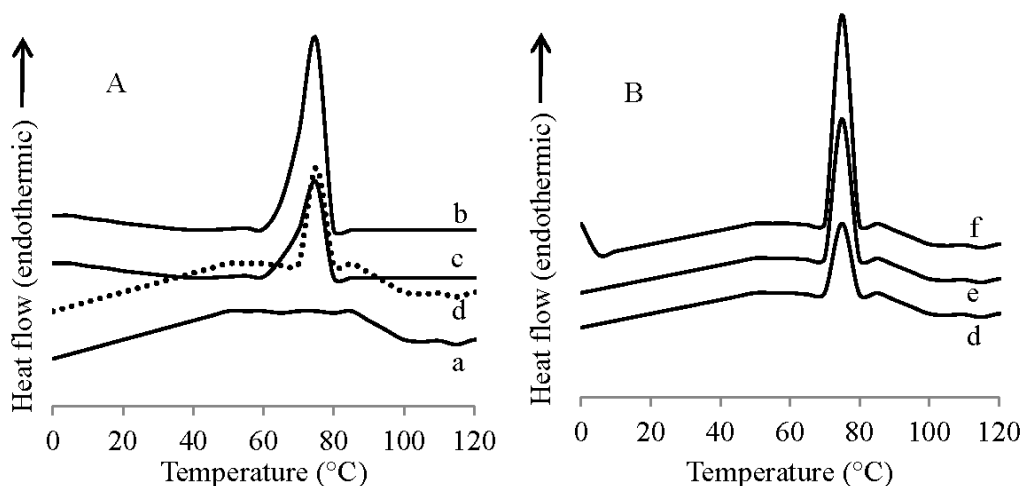


Figure 4. DSC thermogram of unloaded complex coacervate (a), m-INN (b), 1:1:1 physical mixture of CMSP: gelatine: m-INN (c), 30 (d), 45 (e) and 56% w/w (f) m-INN-loaded complex coacervate. (A) represents thermograms of unloaded coacervate (a), m-INN (b), 1:1:1 physical mixture of CMSP: gelatine: m-INN (c) and 30% w/w (d) loaded coacervate. (B) indicates influence of different drug loading in the intensity of crystalline peak.

3.6. Thermogravimetric Analysis

The TGA of CMSP, gelatine and the coacervates are shown in Figure 5a. CMSP has shown a weight loss of 20% at 100–275 °C; this loss in weight is due to loss of moisture. The thermal degradation of CMSP was observed at 275–300 °C, with a 60% weight loss at 600 °C. Gelatine exhibited degradation over a temperature range of 200–400 °C with a net weight loss of 80%. The complex coacervates followed a similar trend as gelatine; however, a slightly slower degradation was observed between 225 and 300 °C due to complexation. Complex coacervate exhibits less degradation than gelatine and CMC in the range of 20–225 °C. The TGA curve of the m-INN (Figure 5b) shows two stages of degradation. The first stage ranges in temperature between 50 and 150 °C, with a weight loss of 10% that is probably due to absorbed moisture and melting. Later, a thermal degradation from 175 to 250 °C, with a weight loss of 100%, was observed that could be due to sublimation [28]. The TGA curve of the m-INN loaded coacervates showed the combination of the coacervate and drug. A relationship between drug loading and weight loss was observed in the TGA of the microcapsules. At 275 °C, an approximate weight loss of 40%, 50% and 60% were observed in microcapsules loaded with 30%, 45% and 56% w/w of the m-INN, respectively. The different decreasing slopes of the TGA curves of various drug-loading amounts indicate that no interaction between the coacervates and the drug is present. Ibuprofen was completely removed during the heating process due to sublimation and thus showed 100% weight loss. However, CMSP and gelatin left residual ashes after degradation and hence showed a residual weight at higher temperatures.

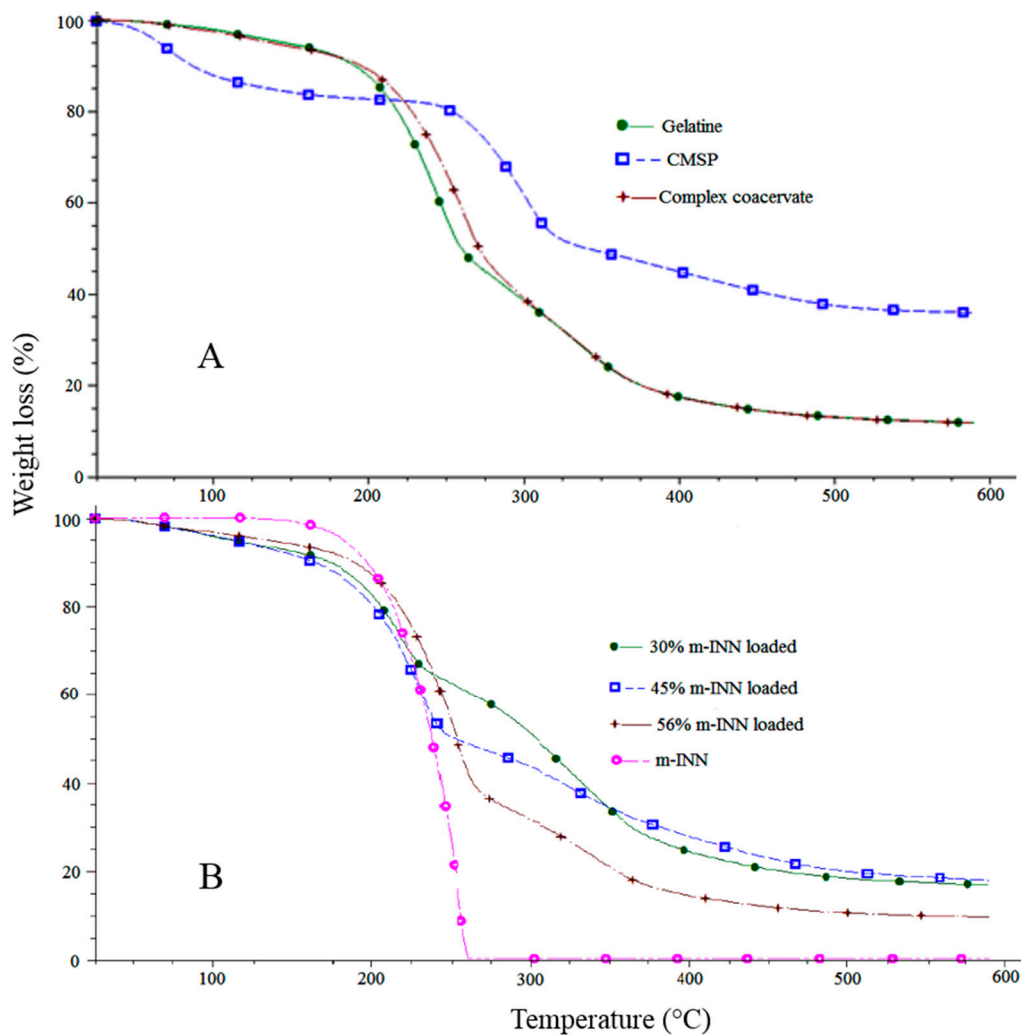


Figure 5. (A) TGA of gelatine, CMSP and unloaded complex coacervates; and (B) TGA of micronized ibuprofen, 30, 45 and 56% *w/w* drug loaded microcapsules.

3.7. Optical Microscopy and FESEM

Photomicrograph (Figure 6a) show native ibuprofen with larger particles. Coacervates unable to encapsulate the native drug particles in the presence of surfactant are shown in Figure 6b. Pictures of micronized ibuprofen and freshly prepared unloaded coacervate are shown in Figure 6c,d, respectively. A picture of coacervate (Figure 6d) reveals the spherical to oval-shaped coacervate formed during phase separation. The incorporation of the m-INN in the newly prepared coacervates is shown in Figure 6e,f. Though the freshly prepared microcapsules appeared to be spherical, the dried one was irregular in shape, as evidenced by FESEM. The irregular shape might be due to the dehydration of the coacervates, which produces a membrane around the drug particles to form microcapsules. FESEM pictures of the microcapsules (Figure S1) are provided in the supplementary document. The surface of the unloaded microcapsule (Figure S1A,B) was smoother than the drug-loaded microcapsule (Figure S1C,D). Crystals of ibuprofen are seen on the surface of drug-loaded microcapsules (Figure S1F).

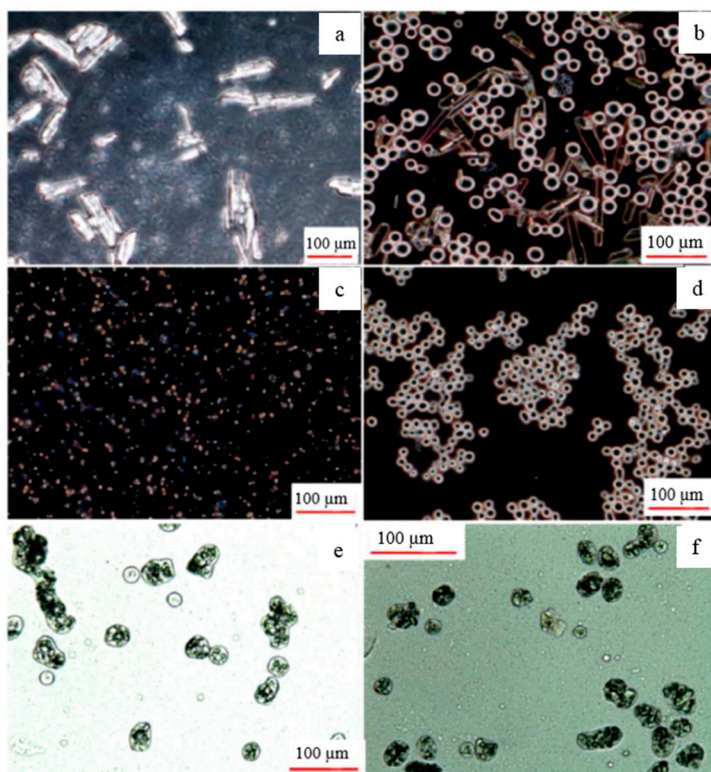


Figure 6. Photomicrographs showing native ibuprofen (a) that is not encapsulated by the coacervate (b) in presence of surfactant; Micronized ibuprofen (c) when added to coacervates without surfactant (d) successfully encapsulated by the coacervates (e,f).

3.8. *In Vitro* Drug Release

The release profiles of ibuprofen from CMSP-gelatine microcapsules are shown in Figure 7. Crosslinking with glutaraldehyde played an important role in hardening and making a compact capsule wall. A decrease in release rate was observed as the concentration of GST increases from 10 to 30 mL (Figure 7A). As shown in Figure 7A, the addition of $AlCl_3$ resulted in much slower release of the drug from the GST cross-linked microcapsules. The CMSP-gelatine microcapsules loaded with 30% drug and cross-linked with GST/ $AlCl_3$ could sustain the release up to 6 h. This sustained release could be due to an increase in extent of cross-linking in the microcapsule wall by the interaction of $AlCl_3$ with CMSP. As indicated in Figure 1, the coacervate has a negative charge due to the excess carboxyl group, which may interact with $AlCl_3$ to provide further cross-linking. A burst release of the drug was observed in all formulations (Figure 7), and the extent of this effect was less in the samples with higher cross-linking. This burst release could be due to surface drugs or poorly encapsulated drug. As shown in Figure 7, the burst release varied from 38% to 60% depending on drug loading and the level of cross-linking. The relative dimensions of wall thickness and the extent of cross-linking in the microcapsules account for the size of the initial burst release [29]. At higher drug loading amounts, the drug may present very near to the surface of the microcapsules due to a smaller wall thickness or poorly encapsulated drug, both of which may explain the burst effect [29–31].

As shown in Table 1, the microcapsules were prepared with increasing quantities of drug with the same quantity of coacervates. The coacervates loaded with a higher amount of drug would

encapsulate the entire drug resulting in a relatively thinner capsule wall [32] than that of the microcapsules loaded with lower drug amounts. This results in a faster diffusion of the drug in highly loaded microcapsules and a less sustained effect [20]. As shown in Figure 7b, 56% of the loaded microcapsules could sustain release for only 90 min. In contrast, formulations with lower drug loading showed a better sustained effect due to relatively thick wall formation because of higher coacervate content with respect to the drug. Devi *et al.* [33] (2012) reported a similar observation in gelatine-sodium alginate complex coacervate loaded with a different level of olive oil.

3.9. Release Kinetics

Data obtained from *in vitro* release studies were fitted to various kinetic equations [19,34]. The kinetic models used are zero order, first order and the Higuchi equation. The following plots were made: Q_t vs. t (zero order); $\log(Q_0 - Q_t)$ vs. t (first-order); Q_t vs. the square root of t (Higuchi), where Q_t is the amount of m-INN released at time t and Q_0 is the initial amount of drug in microcapsules. Furthermore, to determine the mechanism of drug release, the first 60% drug release was fitted to the Korsmeyer-Peppas model.

$$M_t/M_\alpha = kt^n \quad (3)$$

M_t/M_α is the fraction of drug released at time t , k is rate constant and n is the release exponent. The n value is used to characterize different release mechanisms. Higher correlation was observed in first order and Higuchi ($R \geq 0.90$) than in the zero order ($R \leq 0.76$). The highest correlation was observed in the Korsmeyer-Peppas model with an R value above 0.95. The value of the release exponent n was found to be less than 0.39, suggesting Fickian diffusion. All of these parameters indicate that the drug release followed first order kinetics and was regulated by diffusion rather than swelling. Individual values of each formulation are included in the supplementary document (Tables S1 and S2) that is available in the online version of this article.

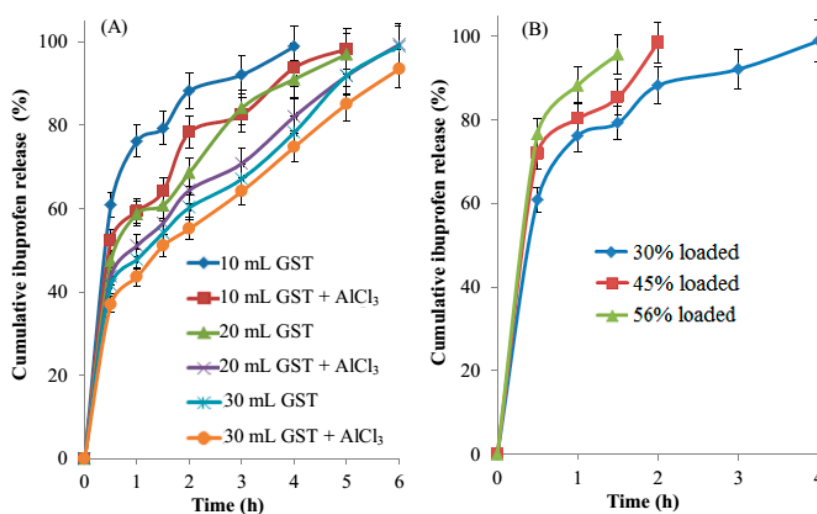


Figure 7. Influence of various cross-linking parameters (A) on the release profile of 30% m-INN loaded microcapsules, in which each point represents an average of three determinations; and the influence of m-INN loading on the release profile (B) of GST cross-linked microcapsules ($n = 3$).

As shown in Figure 7, the effect of aluminum chloride on sustain release was higher in 10-mL GST cross-linked coacervates than 20- and 30-mL GST cross-linked coacervates. This result shows that the effect of GST cross-linking is dominant at its higher concentration. Addition of aluminum chloride sustained 10%–20%, 5%–15%, 5%–8% *w/w* of ibuprofen release from 10, 20, 30 mL GST cross-linked coacervates, respectively. Because the coacervates were highly cross-linked at high GST levels, aluminum chloride was unable to penetrate the coacervate for further cross-linking.

3.10. Residual Glutaraldehyde

Because glutaraldehyde is known for toxicity, the microcapsules must be free from residual glutaraldehyde, which could cause irritation and inflammation [21]. The American Congress of Government Industrial Hygienists [35] lowered their limit to 0.05 ppm. United States Pharmacopeia classifies toluene as a class 2 residual solvent and its presence should be less than 890 ppm. Gas chromatography analysis qualitatively confirms the absence of residual glutaraldehyde and toluene in the microcapsules. A representative gas chromatogram in the supplementary document (Figure S2) shows peaks of isopropanol, toluene and glutaraldehyde in the physical mixture of these substances. The peaks of toluene and glutaraldehyde were absent in the chromatogram of formulations, suggesting the absence of these materials. The toluene might have removed while washing with isopropanol as well as during drying. The quenching agent sodium metabisulfite, used during the recovery process, effectively removed the unreacted glutaraldehyde from the microcapsules. We have also reported similar observation in a previous publication [21].

4. Conclusions

The present work reports a new complex coacervation microcapsule based on CMSP-gelatine for sustained drug delivery. The AlCl_3 further sustained the drug release from glutaraldehyde cross-linked coacervates. The dual cross-linking could be optimized to obtain the required drug release profile, which was found to be diffusion controlled. The same method could encapsulate biological material, as a less harsh environment is used in the manufacturing process. Because CMSP is obtained from waste biomass of Malaysian sago industries, its synthesis and application in the microencapsulation process will reduce environmental pollution and sustain a green environment.

Supplementary Materials

Supplementary materials can be accessed at: <http://www.mdpi.com/2073-4360/7/6/1088/s1>.

Acknowledgments

The synthesis of CMSP from sago biomass was funded by the Ministry of Higher Education through Exploratory Research grant (ERGS) (ERGS/1/2012/TK04/MUSM/03/1). The remaining work supported by a seed grant (BCHH-SS-6-02-2010) obtained from Monash University, Malaysia. APC of this manuscript was supported by School of Pharmacy, Monash, Malaysia.

Author Contributions

Pushpamalar Janarthanan has contributed to the synthesis and the characterization of CMSP from Sago biomass; Thenapakiam Sathasivam has conducted all the experiments and analyzed the results; Anand Kumar Veeramachineni contributed to the characterization of the microcapsules; and Saravanan Muniyandy has written the manuscript and contributed in the development and characterization of complex coacervates.

Conflicts of Interest

The authors declare no conflict of interest.

References

1. Pushpamalar, V.; Langford, S.; Ahmad, M.; Lim, Y. Optimization of reaction conditions for preparing carboxymethyl cellulose from sago waste. *Carbohydr. Polym.* **2006**, *64*, 312–318.
2. Pushpamalar, V.; Langford, S.; Ahmad, M.; Hashim, K.; Lim, Y. Absorption characterization of Ca^{2+} , Na^{+} , and K^{+} on irradiation cross-linked carboxymethyl sago pulp hydrogel. *J. Appl. Polym. Sci.* **2013**, *128*, 1828–1833.
3. Pushpamalar, V. *Preparation and Characterisation of Carboxymethyl Cellulose and Carboxymethyl Cellulose Hydrogels from Sago Waste*; Monash University: Clayton, Australia, 2010.
4. Thenapakiam, S.; Kumar, D.G.; Pushpamalar, J.; Saravanan, M. Aluminium and radiation cross-linked carboxymethyl sago pulp beads for colon targeted delivery. *Carbohydr. Polym.* **2013**, *94*, 356–363.
5. Deasy, P.B. *Microencapsulation and Related Drug Processes*; Marcel Dekker Inc.: New York, NY, USA, 1984.
6. Polk, A.; Amsden, B.; de Yao, K.; Peng, T.; Goosen, M. Controlled release of albumin from chitosan—Alginate microcapsules. *J. Pharm. Sci.* **1994**, *83*, 178–185.
7. Wen, S.; Alexander, H.; Inchikel, A.; Stevenson, W.T. Microcapsules through polymer complexation: Part 3: Encapsulation and culture of human burkitt lymphoma cells *in vitro*. *Biomaterials* **1995**, *16*, 325–335.
8. De Kruif, C.G.; Weinbreck, F.; de Vries, R. Complex coacervation of proteins and anionic polysaccharides. *Curr. Opin. Colloid Interface Sci.* **2004**, *9*, 340–349.
9. Saravanan, M.; Rao, K.P. Pectin–gelatin and alginate–gelatin complex coacervation for controlled drug delivery: Influence of anionic polysaccharides and drugs being encapsulated on physicochemical properties of microcapsules. *Carbohydr. Polym.* **2010**, *80*, 808–816.
10. Harada, A.; Kataoka, K. Formation of polyion complex micelles in an aqueous milieu from a pair of oppositely-charged block copolymers with poly(ethylene glycol) segments. *Macromolecules* **1995**, *28*, 5294–5299.
11. Harada, A.; Kataoka, K. Pronounced activity of enzymes through the incorporation into the core of polyion complex micelles made from charged block copolymers. *J. Control. Release* **2001**, *72*, 85–91.

12. Black, K.A.; Priftis, D.; Perry, S.L.; Yip, J.; Byun, W.Y.; Tirrell, M. Protein encapsulation via polypeptide complex coacervation. *ACS Macro Lett.* **2014**, *3*, 1088–1091.
13. Perry, S.L.; Li, Y.; Priftis, D.; Leon, L.; Tirrell, M. The effect of salt on the complex coacervation of vinyl polyelectrolytes. *Polymers* **2014**, *6*, 1756–1772.
14. Chollakup, R.; Beck, J.B.; Dirnberger, K.; Tirrell, M.; Eisenbach, C.D. Polyelectrolyte molecular weight and salt effects on the phase behavior and coacervation of aqueous solutions of poly(acrylic acid) sodium salt and poly(allylamine) hydrochloride. *Macromolecules* **2013**, *46*, 2376–2390.
15. Wong, R.C.; Kang, S.; Heezen, J.L.; Voorhees, J.J.; Ellis, C.N. Oral ibuprofen and tetracycline for the treatment of acne vulgaris. *J. Am. Acad. Dermatol.* **1984**, *11*, 1076–1081.
16. Curhan, S.G.; Eavey, R.; Shargorodsky, J.; Curhan, G.C. Analgesic use and the risk of hearing loss in men. *Am. J. Med.* **2010**, *123*, 231–237.
17. Hippisley-Cox, J.; Coupland, C. Risk of myocardial infarction in patients taking cyclo-oxygenase-2 inhibitors or conventional non-steroidal anti-inflammatory drugs: Population based nested case-control analysis. *BMJ* **2005**, *330*, 1366
18. Mansouri, M.; Pouretedal, H.R.; Vosoughi, V. Preparation and characterization of Ibuprofen nanoparticles by using solvent/antisolvent precipitation. *Open Conf. Proc. J.* **2011**, *2*, 88–94.
19. Saravanan, M.; Bhaskar, K.; Rao, G.S.; Dhanaraju, M. Ibuprofen-loaded ethylcellulose/polystyrene microspheres: An approach to get prolonged drug release with reduced burst effect and low ethylcellulose content. *J. Microencapsul.* **2003**, *20*, 289–302.
20. Boppana, R.; Kulkarni, R.V.; Mutalik, S.S.; Setty, C.M.; Sa, B. Interpenetrating network hydrogel beads of carboxymethylcellulose and egg albumin for controlled release of lipid lowering drug. *J. Microencapsul.* **2010**, *27*, 337–344.
21. Saravanan, M.; Bhaskar, K.; Maharajan, G.; Pillai, K.S. Development of gelatin microspheres loaded with diclofenac sodium for intra-articular administration. *J. Drug Target.* **2011**, *19*, 96–103.
22. Barbucci, R.; Magnani, A.; Consumi, M. Swelling behavior of carboxymethylcellulose hydrogels in relation to cross-linking, pH, and charge density. *Macromolecules* **2000**, *33*, 7475–7480.
23. Charpentier-Valenza, D.; Merle, L.; Mocanu, G.; Picton, L.; Muller, G. Rheological properties of hydrophobically modified carboxymethylcelluloses. *Carbohydr. Polym.* **2005**, *60*, 87–94.
24. Wang, M.; Xu, L.; Hu, H.; Zhai, M.; Peng, J.; Nho, Y.; Li, J.; Wei, G. Radiation synthesis of PVP/CMC hydrogels as wound dressing. *Nucl. Instrum. Methods. Phys. Res. Section B* **2007**, *265*, 385–389.
25. Muyonga, J.; Cole, C.; Duodu, K. Fourier transform infrared (FTIR) spectroscopic study of acid soluble collagen and gelatin from skins and bones of young and adult Nile perch (*Lates niloticus*). *Food Chem.* **2004**, *86*, 325–332.
26. Garrigues, S.; Gallignani, M.; de la Guardia, M. FIA-FT-IR determination of ibuprofen in pharmaceuticals. *Talanta* **1993**, *40*, 89–93.
27. Han, X.; Ghoroi, C.; To, D.; Chen, Y.; Davé, R. Simultaneous micronization and surface modification for improvement of flow and dissolution of drug particles. *Int. J. Pharm.* **2011**, *415*, 185–195.
28. Garnero, C.; Aloisio, C.; Longhi, M. Ibuprofen-maltodextrin interaction: Study of enantiomeric recognition and complex characterization. *Pharmacol. Pharm.* **2013**, *4*, 18.

29. Huang, X.; Brazel, C.S. On the importance and mechanisms of burst release in matrix-controlled drug delivery systems. *J. Control. Release* **2001**, *73*, 121–136.
30. Batycky, R.P.; Hanes, J.; Langer, R.; Edwards, D.A. A theoretical model of erosion and macromolecular drug release from biodegrading microspheres. *J. Pharm. Sci.* **1997**, *86*, 1464–1477.
31. Brazel, C.S.; Peppas, N.A. Mechanisms of solute and drug transport in relaxing, swellable, hydrophilic glassy polymers. *Polymer* **1999**, *40*, 3383–3398.
32. Hedayati, R.; Jahanshahi, M.; Attar, H. Fabrication and characterization of albumin-acacia nanoparticles based on complex coacervation as potent nanocarrier. *J. Chem. Technol. Biotechnol.* **2012**, *87*, 1401–1408.
33. Devi, N.; Hazarika, D.; Deka, C.; Kakati, D. Study of complex coacervation of gelatin A and sodium alginate for microencapsulation of olive oil. *J. Macromol. Sci. Part A* **2012**, *49*, 936–945.
34. Costa, P.; Lobo, J.M.S. Modeling and comparison of dissolution profiles. *Eur. J. Pharm. Sci.* **2001**, *13*, 123–133.
35. Smilanick, J.L.; Sorenson, D.; Verduzco, G.; Ames, Z.R.; Mansour, M. Evaluation of disinfectants for citrus packinghouses. *Citrograph* **2011**, *49*, 50–55.

© 2015 by the authors; licensee MDPI, Basel, Switzerland. This article is an open access article distributed under the terms and conditions of the Creative Commons Attribution license (<http://creativecommons.org/licenses/by/4.0/>).